

## Structure Prediction of Bis(amino acidato)copper(II) Complexes with a New Force Field for Molecular Modeling

Jasmina Sabolović<sup>\*,†</sup> and Vjeran Gomzi<sup>‡</sup>

*Institute for Medical Research and Occupational Health, Ksaverska cesta 2, P.O. Box 291, HR-10001 Zagreb, Croatia, and Ruđer Bošković Institute, Bijenička cesta 54, HR-10000 Zagreb, Croatia*

Received January 12, 2009

**Abstract:** This article presents a new force field whose parameterization was based on experimental crystal data and quantum chemically obtained vacuum structures of a series of copper(II) complexes with aliphatic  $\alpha$ -amino acids and their *N*-alkyl derivatives, along with the SPC/E water model. The ability of the new force field to reproduce and predict the structural properties of the copper(II) complexes in the gas phase, in simulated crystalline surroundings, and solvated in water is examined. Molecular dynamics (MD) simulations with the new force field yielded time-average structural coordinates of bis(glycinato)copper(II) [the only one of 25 modeled bis(amino acidato)copper(II) systems with published experimental structural data in aqueous solution at room temperature] within the experimental error values. The study of the cis–trans isomerization of bis(glycinato)copper(II) in aqueous medium at 300 K using the quantum chemical polarized continuum model revealed a small energy difference (5 kJ mol<sup>-1</sup>) between the solvated cis and trans minima, in line with the MD energy estimations. The new force field proved promising in predicting the association of the complexes in aqueous solution and formation of a nucleus of crystallization.

### Introduction

Copper, like other essential transition metals (iron, zinc, cobalt, manganese), is present in many biological fluids as the free ion or complexed in metalloproteins and low-molecular-weight complexes with peptides and amino acids.<sup>1–3</sup> In healthy organisms, physiological copper concentrations are maintained by a number of homeostatic mechanisms, such as absorption regulation, cellular uptake and efflux, intracellular transport, sequestration/storage, and copper excretion from the body.<sup>4,5</sup> Exposure to excess copper through an accident, occupational hazard, environmental contamination, or human genetic disorder (Menkes disease, occipital horn syndrome, or Wilson disease)<sup>2,4</sup> causes copper overload, disruptions to normal copper homeostasis, copper-

induced oxidative damage, and toxic effects in organs.<sup>5</sup> From available data on human exposures worldwide, there is a greater risk of health effects from copper deficiency (which might also increase cellular susceptibility to oxidative damage)<sup>5</sup> than from excess copper intake.<sup>6</sup>

Copper is required as a cofactor for structural and catalytic activity in a number of enzymes (e.g., cytochrome *c* oxidase, lysyl oxidase, tyrosinase, superoxide dismutase).<sup>3</sup> An analysis of the types and frequencies of amino acid residues involved in the coordination of metal ions in metalloproteins that was performed on a set of structures extracted from the Protein Data Bank in October 2007 showed that copper preferred the coordination number 4 and that it was most often coordinated by histidine imidazole nitrogen atom, followed by cysteine sulfur atom.<sup>7</sup> L-Histidine was also identified as the predominant amino acid bound to copper(II) in bis-(L-histidinato)copper(II) (with imidazole nitrogen, amino nitrogen, and carboxylato oxygen donor atoms) and in mixed

\* Corresponding author e-mail: jasmina.sabolovic@imi.hr; phone: +385 1 4673 188; fax: +385 1 4673 303.

<sup>†</sup> Institute for Medical Research and Occupational Health.

<sup>‡</sup> Ruđer Bošković Institute.

copper(II) complexes with other L-amino acids in human blood serum.<sup>3</sup>

Whereas metalloproteins are relatively easy to isolate, low-molecular-weight complexes form parts of multicomponent systems with different complexing species in solution. Most spectroscopic and electrochemical methods allow identification of the prevailing complexes and their stability constants in solutions, but they provide no structural information.<sup>3,8–19</sup> For instance, trans and cis isomers for a number of bis(amino acidato)copper(II) complexes were confirmed to exist in aqueous solution by the <sup>14</sup>N superhyperfine structure in electron paramagnetic resonance (EPR) spectra without details on their geometry.<sup>16–19</sup> Some structural data only for bis(glycinato)copper(II), Cu(Gly)<sub>2</sub>, in aqueous solution were obtained by X-ray absorption spectroscopy,<sup>20</sup> whereas for other copper(II) chelates with aliphatic  $\alpha$ -amino acids and their *N*-alkyl derivatives, the only experimentally available structures are those determined by X-ray and neutron diffraction studies.<sup>21–43</sup>

The structural properties can be predicted and reproduced using the molecular modeling methods, for example, molecular dynamics (MD) simulations. However, prerequisite for MD calculations is a reliable molecular mechanics (MM) force field.<sup>44</sup> To the best of our knowledge, such a force field has not yet been reported for low-molecular-weight transition metal complexes with amino acids.

The development of MM models and force fields for transition metal complexes has been complicated by the large number of transition metal elements; system-specific metal–ligand interactions; and the diversity of oxidation states, coordination numbers, and geometrical shapes around metal centers, together with the lack of experimental data for force field parameterization.<sup>45–49</sup> Both the development of quantum chemical methods and the expansion of computer power have contributed to an increase of quantum chemical data suitable for force field parameterization and/or validation of the MM results during past decade. Next, we mention several parameterization studies involving copper complexes.

The polarizable MM procedure SIBFA (sum of interactions between fragments ab initio computed) was used to treat copper(II) in complexes with HIV-1 protease inhibitors, *N*<sub>1</sub>-(4-methyl-2-pyridyl)-2,3,6-trimethoxybenzamide, and *N*<sub>2</sub>-(2-methoxybenzyl)-2-quinolinecarboxamide to study the structural and energetic aspects, as well as to compare the relative stability of the complexes.<sup>50</sup>

A ReaxFF reactive force field, in which the parameters were fitted to a substantial database of quantum chemical data (binding energies, ground-state systems, full reactive pathways), was developed for reactions involving carbon materials and transition metal atoms, including copper, usually employed in catalytic transformations.<sup>51</sup> The force field was applied for high-temperature MD simulations in the presence of metal atoms and carbon fragments, which demonstrated different catalytic abilities of the metals in the formation of small polycyclic structures serving as nucleation points for further nanostructure formation.

Given the need for an accurate and general force field for type 1 copper binding sites in the copper(II) form of blue copper proteins involved in electron transport, Comba and

Remenyi<sup>52,53</sup> based the force field parameterization on potential energy curves [computed energy vs bond distance (valence angle) in the gas phase by density functional theory (DFT)] of the model compound [Cu(imidazole)<sub>2</sub>(SCH<sub>3</sub>)-S(CH<sub>3</sub>)<sub>2</sub>]<sup>+</sup>. DFT curves were used to fit corresponding MM curves by least-squares fitting and thus to develop the force field parameters.

The ligand-field MM (LFMM) model was also applied to model compounds for the oxidized type 1 copper center.<sup>54,55</sup> The parameters were developed on the basis of DFT geometries optimized in vacuo for the homoleptic model compounds [Cu(SCH<sub>3</sub>)<sub>4</sub>]<sup>2-</sup>, [Cu(S(CH<sub>3</sub>)<sub>2</sub>)<sub>4</sub>]<sup>2+</sup>, [Cu(imidazole)<sub>4</sub>]<sup>2+</sup>, and [Cu(O=CH<sub>2</sub>)<sub>4</sub>]<sup>2+</sup>; validated on the active-site model complex [Cu(imidazole)<sub>2</sub>(SCH<sub>3</sub>)(S(CH<sub>3</sub>)<sub>2</sub>)]<sup>+</sup>; and then applied for modeling of the active sites of 24 crystallographically characterized blue copper proteins surrounded with a layer of water molecules.<sup>55</sup> The development and applications of the LFMM model for transition metal complexes were summarized in a recent review.<sup>56</sup>

We have developed MM models and force fields for copper(II) complexes with aliphatic  $\alpha$ -amino acids with the aim of reproducing and predicting the properties of the whole class of bis(amino acidato)copper(II) complexes (by subsequent inclusion of other amino acids in the force field parameterization) in different environments (vacuum, crystal, solution).<sup>31,57–59</sup> To achieve this aim, the environmental effects are calculated explicitly; that is, the same set of potential energy functions and their empirical parameters are used both for modeling the isolated systems and for simulating condensed phases. In the latter case, the effects of the surrounding environment of a molecule (such as crystal and solution) are calculated explicitly by including the environment in the calculations. The approach affects the force field parameterization based on available experimental crystal data and the results of quantum chemical studies.<sup>31,58,59</sup>

The experimental crystal and molecular structures of anhydrous and aqua copper(II) complexes with aliphatic  $\alpha$ -amino acids and their *N*-alkyl derivatives<sup>21–43</sup> differ with respect to the copper(II) coordination polyhedron geometries and intermolecular interactions, which makes this class of complexes challenging for modeling. Copper(II), as a Jahn–Teller (or pseudo-Jahn–Teller) center,<sup>60</sup> adopts diverse coordination geometries such as irregular square-planar, distorted planar, flattened tetrahedral, elongated octahedral, distorted octahedral, and irregular or distorted square pyramidal in the crystal state.<sup>59</sup> In addition to the usual intermolecular van der Waals and hydrogen-bonding interactions, copper(II) can have weak coordinative bonding with an axially placed water oxygen atom and/or carbonyl oxygen atom from an adjacent molecule in the crystal lattice. The exceptions are truly four-coordinate trans copper(II) chelates with *N,N*-dialkylated valine,<sup>21,24</sup> isoleucine,<sup>23</sup> and alanine,<sup>22,31</sup> bonded only via van der Waals interactions. Any newly solved crystal and molecular structure of a copper(II) chelate with amino acids is very welcome because it enlarges the collection of knowledge about structural properties. Such an example is the recent X-ray crystal and molecular structure of anhydrous *trans*-bis(*N,N*-diethylglycinato)copper(II), Cu(Et<sub>2</sub>Gly)<sub>2</sub>, in which a relatively short copper-to-axial-

carbonyl-oxygen distance of 2.312 Å was found,<sup>37</sup> whereas in other anhydrous trans copper(II) amino acidates, this distance spans the range from 2.6 to 3.1 Å.<sup>59</sup>

Although many quantum chemical studies on model compounds of metal-binding sites in copper metalloproteins have been performed,<sup>52,54,61,62</sup> only a few have investigated bis complexes of copper(II) with amino acids.<sup>58,59,63–65</sup> Quantum chemical calculations of electronic and geometrical properties,<sup>63–65</sup> the gas-phase potential energy profile for the cis–trans isomerization reaction,<sup>64</sup> water molecules' bindings,<sup>59,63,65</sup> and reaction rate constants<sup>64,65</sup> have been done for Cu(Gly)<sub>2</sub>. The quantum chemical calculations of equilibrium structures for three anhydrous copper(II) complexes with L-alanine, L-leucine, and L-*N,N*-dimethylvaline<sup>58</sup> and four aquabis copper(II) glycinate complexes<sup>59</sup> revealed that the experimental crystal and ab initio derived vacuum geometries differ. Their structure comparisons clarify the influence of the crystal environment on the copper(II) coordination geometry and overall complex geometry, and the modeling of the impact of the intermolecular interactions on the geometry changes represents an additional challenge.<sup>31,37,38,58,59</sup>

Although our most recent force field, FFW,<sup>31,59</sup> proved as reliable for modeling anhydrous and aquabis(amino acidato)copper(II) complexes in vacuo and in the crystal,<sup>37,38,59</sup> the empirical parameters of the nonbonded potential energy functions for the water molecule's oxygen and hydrogen atoms used in FFW yielded an incorrect water density (around 1140 kg m<sup>-3</sup>) and a too-compact system with almost no diffusion of water molecules in the MD simulations. Specifically, the parameters yielded forces between the water molecules that were too attractive; this did not cause problems in hypothetical motionless equilibrium structures calculated by MM gas-phase and in-crystal simulations, but it did cause problems in MD calculations. Therefore, using the empirical parameters of the SPC/E water model,<sup>66</sup> the FFW force field was reparametrized in an exhaustive effort, and a set of force field empirical parameters equally applicable for vacuum, crystal, and aqueous solution was derived. This article presents the new force field and discusses its ability to reproduce and predict the properties of the copper(II) class of compounds in vacuo and in the crystal by MM calculations, as well as in aqueous solution by MD simulations. The MD results were verified by comparison with the quantum chemical results obtained within the polarized continuum model<sup>67</sup> (PCM) approximation. In addition, standard transition state theory was applied to PCM energies to gain insight into the cis–trans isomerization reaction of Cu(Gly)<sub>2</sub> in aqueous solution at 300 K.

## Methods

**MM Model and Calculations.** The conformational (strain) potential energy was calculated from the following basic formula

$$V_{\text{strain}} = V(b) + V(\theta) + V(\varphi) + V(\chi) + V_{\text{LJ}} + V_{\text{Coulomb}} \\ = \sum_{\text{bonds}} D_e (e^{-2\alpha(b-b_0)} - 2e^{-\alpha(b-b_0)} + 1) + \frac{1}{2} \sum_{\text{valence angles}} k_\theta (\theta - \theta_0)^2 + \frac{1}{2} \sum_{\text{torsion angles}} V_\varphi (1 \pm \cos n\varphi) + \frac{1}{2} \sum_{\text{out-of-plane angles}} k_\chi \chi^2 + \sum_{i < j} (A_i A_j r_{ij}^{-12} - B_i B_j r_{ij}^{-6}) + \sum_{l < m} q_l q_m r_{lm}^{-1} \quad (1)$$

Here,  $b$ ,  $\theta$ ,  $\varphi$ ,  $\chi$ , and  $r$  are the bond length; the valence, torsion, and out-of-plane angles, and the nonbonded distance, respectively.  $D_e$ ,  $\alpha$ , and  $b_0$  are empirical parameters for bond stretching (a Morse function);  $k_\theta$  and  $\theta_0$  are empirical parameters for valence-angle bending; and  $k_\chi$  is an empirical parameter for the out-of-plane deformational potential for the carboxyl groups. Torsional interactions are specified with  $V_\varphi$  and  $n$  (height and multiplicity of the torsional barrier, respectively). One torsion per bond was calculated.  $A$  and  $B$  are one-atom empirical parameters for the van der Waals interactions (a Lennard-Jones 12–6 function).  $q$  is a charge parameter. Intramolecular interactions between atoms separated by three or more bonds were considered nonbonded and were calculated with the Lennard-Jones ( $V_{\text{LJ}}$ ) and electrostatic ( $V_{\text{Coulomb,NB}}$ ) potentials, respectively.

The interactions within the copper(II) coordination sphere were modeled using the Morse potential between the copper and ligand donor atoms (two amino nitrogen and two carboxylato oxygen atoms); the repulsive electrostatic potential between the four donor atoms ( $V_{\text{Coulomb,1-3}}$ ); and a torsion-like potential dependent on the “torsion” angle O–N–N–O, with two minima at 0° and 180° that correspond to the cis- and the trans-planar CuN<sub>2</sub>O<sub>2</sub> configurations, respectively.<sup>31</sup> It is a model without any explicit valence-angle bending potential for the angles around copper.<sup>31,57–59</sup>

The interactions between the water molecule's oxygen and hydrogen atoms and the atoms of a bis(amino acidato)copper(II) complex were calculated with the Lennard-Jones 12–6 and electrostatic potentials regardless of the water molecule position around the copper(II) complex.<sup>59</sup>

All MM calculations were performed using the modified version<sup>68</sup> of the Lyngby version of the CFF program for conformational analysis.<sup>69–71</sup> The conformational potential energy was minimized for an isolated molecular system (in vacuo or a gas-phase approximation) and for a molecule surrounded by other molecules in the simulated crystal lattice (a condensed-phase approximation). The intermolecular atom–atom interactions were calculated using the same functional forms (Lennard-Jones 12–6 function and Coulombic potential) and empirical parameters as for the intramolecular nonbonded interactions. The crystal simulations were carried out using the Williams variant of the Ewald lattice summation method<sup>72,73</sup> with a spherical and abrupt cutoff limit of 14 Å, and convergence constants of 0.2 Å<sup>-1</sup>, 0.2 Å<sup>-1</sup>, and 0.0 for Coulomb, dispersion, and repulsion lattice summation terms, respectively. A detailed description of the crystal simulations is given elsewhere.<sup>31,37,73</sup>

In the Lyngby-CFF program, the input charge parameters are used for an assignment of fractional atomic charges.<sup>71</sup>



The assignment is done by a special charge redistribution algorithm, which keeps the total charge of the molecules neutral and distributes the charge values in a manner supposed to mimic *ab initio* results. The charge distribution routine was modified<sup>31</sup> to obtain the assigned fractional charges for the copper(II) chelates with amino acids close to the charges resulting from the natural population analysis<sup>74</sup> (NPA). The reason for selecting NPA charges as a guideline to the charge parameter values has been given elsewhere.<sup>58,68</sup> Our choice of the potential energy functions was based on available options in the Lyngby-CFF program, and the combination of the Lennard-Jones 12–6 and Coulombic potentials is the only one implemented for intermolecular atom–atom interactions in the crystal simulator of the program. Hence, the force field developed belongs to the class of nonpolarizable fixed-charge force fields.<sup>75</sup>

The empirical parameters of the potential energy functions were determined by combining trial-and-error guesses with the optimization algorithm, which was a variant of the general least-squares method (the Levenberg–Marquardt algorithm).<sup>70,71</sup>

**MD Simulations.** The simulations were performed using the program package Gromacs, version 3.2.1,<sup>76,77</sup> with the new MM force field FFWa-SPCE<sup>78</sup> (see MM Force Field Parameterization section) developed for copper(II) complexes with aliphatic amino acids. MD calculations were carried out for *trans* and *cis* isomers of Cu(Gly)<sub>2</sub> separately, and also for four Cu(Gly)<sub>2</sub> molecules. One Cu(Gly)<sub>2</sub> and four Cu(Gly)<sub>2</sub> molecules were solvated in rectangular boxes containing 2159 and 5457 water molecules, respectively, and equilibrated for 500 ps. Two nanoseconds of the productive MD phase was accomplished under constant temperature and pressure (298.15 K and 1 bar) using Berendsen T-coupling ( $\tau_T = 0.1$  ps) and Berendsen p-coupling ( $\tau_p = 0.5$  ps).<sup>79</sup> The time step was 1 fs. The water molecules' geometry was constrained by the SETTLE procedure,<sup>80</sup> whereas all Cu(Gly)<sub>2</sub> degrees of freedom were relaxed during the MD simulations. A cutoff limit of 1.5 nm was applied for the calculations of Coulomb and Lennard-Jones 12–6 interactions. The cutoff distance for the short-range neighbor list was set to 1.0 nm.

**Quantum Chemical Calculations.** Geometries and single-point energies of the stationary points of Cu(Gly)<sub>2</sub> [i.e., *trans* and *cis* minima, as well as a transition state (TS) structure] in the gas phase and in aqueous solution were investigated by the unrestricted B3LYP hybrid density functional method<sup>81–84</sup> using the LanL2DZ double- $\xi$  basis set<sup>85</sup> to which an additional set of polarization functions<sup>86</sup> on heavy atoms except copper was added. In addition, diffuse functions<sup>87</sup> were added for the oxygen, nitrogen, and carbon atoms. Through the use of the aforementioned basis set, the effective core potentials of Hay and Wadt<sup>88–90</sup> were used to describe the shielding effects of the electrons in copper inner shells. The basis set used is denoted as B3LYP/LanL2DZ{D95v+(d)} throughout this article. All quantum chemical calculations were performed using the Gaussian 03 package program.<sup>91</sup> The choice of the B3LYP method and the basis set used was based on previous studies of the energies and geometries of copper(II)-glycinato systems.<sup>59,63–65</sup>

They yielded values similar to those obtained by a higher-level theory method [G3(MP2)-B3] and thus indicated the qualitatively correct behavior of the lower-level method.<sup>64</sup>

The PCM of Tomasi and co-workers,<sup>67</sup> modified by Barone and co-workers,<sup>92</sup> was used to describe the effects of the aqueous medium in the self-consistent reaction field (SCRF) calculations. The environmental temperature was set to 300 K. The water solvent was specified by the dielectric constant of 78.39. The united-atom topological model was applied to solvent radii optimized for the PBE0/6-31G(d) level of theory.<sup>93–95</sup>

The initial atom positions for geometry optimizations of the *cis* and *trans* minima and TS structure of Cu(Gly)<sub>2</sub> were the Cartesian coordinates of the stationary points obtained from the quantum chemical gas-phase calculations.<sup>64</sup> The TS structure in aqueous solution at room temperature was successfully calculated only upon using a “good enough” initial guess and by applying the synchronous transit-guided quasi-Newton (STQN) method implemented in programs invoked using the QST3 keyword.<sup>96,97</sup> The optimized geometries of the stationary points were verified by frequency calculations to be those of the required optimization state (TS structure or energy minimum). The energies were calculated using the same level of the theory and basis set. Full geometry optimizations of the gas-phase and TS structures obtained in solution were performed to check the optimization process itself, as well as to verify whether the two isomer structures were accessible from the presumed TS structure.

**Calculation of the Reaction Rate Constants.** To evaluate the reaction rates of the *cis*–*trans* isomerization process in water solution (given that, to the best of our knowledge, there are no experimental data on these reaction rate constants) to the gas phase, we applied the equations from standard transition state theory

$$k_{\text{cis} \rightarrow \text{trans}} = \frac{k_B T}{h} \exp\left(-\frac{\Delta G_{\text{TS} \rightarrow \text{cis}}}{RT}\right) \quad (2a)$$

$$k_{\text{trans} \rightarrow \text{cis}} = \frac{k_B T}{h} \exp\left(-\frac{\Delta G_{\text{TS} \rightarrow \text{trans}}}{RT}\right) \quad (2b)$$

where  $\Delta G_{\text{TS} \rightarrow \text{cis}}$  and  $\Delta G_{\text{TS} \rightarrow \text{trans}}$  represent respective quantum chemically estimated Gibbs free energy differences between the TS structure and the *cis* and *trans* minima,  $h$  is Planck's constant,  $k_B$  is the Boltzmann constant,  $R$  is the gas constant, and the temperature ( $T$ ) is 300 K. The thermal correction to the Gibbs free energy was calculated by adding the zero-point vibrational energy plus thermal rotational–vibrational free energy to the Gibbs free energy at temperature  $T$  obtained from the potential energy in the standard way.<sup>91</sup>

## Results and Discussion

**MM Force Field Parameterization.** The force field FFW,<sup>31,59</sup> developed for anhydrous and aqua copper(II) chelates with aliphatic  $\alpha$ -amino acids with *trans*- and *cis*-CuN<sub>2</sub>O<sub>2</sub> coordination polyhedra, was taken as the initial empirical parameter set for parameter optimization. The empirical parameters of the SPC/E water model<sup>166</sup> were used

to model the interactions of the water molecule's oxygen and hydrogen atoms. As the SPC/E water model uses a harmonic approximation for the bond stretching potential, we fitted the  $D_e$ ,  $\alpha$ , and  $b_0$  empirical parameters of the Morse potential for the  $O_W-H$  bond length (where  $O_W$  denotes the water oxygen atom) to fulfill the relation<sup>69</sup>  $k_b = 2D_e\alpha^2$  (where  $k_b$  is the empirical parameter of the quadratic function for the  $O_W-H$  bond in the SPC/E model) and to yield average  $O_W-H$  bonds equal to 1.0 Å (Table 1). The empirical parameters  $k_\theta$  and  $\theta_0$  for  $H-O_W-H$  valence-angle bending,  $A$  and  $B$  for the Lennard-Jones potential for  $O_W$  and  $H(O_W)$  (Table 1), and the partial charges  $[-0.8476e$  and  $0.4238e$  for  $O_W$  and  $H(O_W)$ , respectively] were taken to be the same as in SPC/E and were held constant during the force field parameterization.

The force field parameterization procedure was the same as for the FFW force field; specifically, it was based on the experimental crystal and molecular structures and the quantum chemical B3LYP minimum vacuum structures and NPA charges.<sup>59</sup>

The modeling included 14 anhydrous and 11 aqua copper(II) amino acid complexes with the same atom types. All of the molecules are electrically neutral. Eleven of them have *trans*- and four have *cis*- $N_2O_2$  coordination to the copper(II).

The empirical parameters were optimized with respect to the experimental data (bond lengths, valence and torsion angles, and unit cell dimensions) of the following seven anhydrous and six aqua copper(II) complexes: *trans*-bis(L-*N,N*-dimethylvalinato)copper(II)<sup>21</sup> [ $Cu(L-Me_2Val)_2$ ], *trans*-bis(D,L-*N,N*-diethylalaninato)copper(II)<sup>22</sup> [ $Cu(D,L-Et_2Ala)_2$ ], *trans*-bis(L-leucinato)copper(II)<sup>26</sup> [ $Cu(L-Leu)_2$ ], *trans*-bis(D,L-2-aminobutyrate)copper(II)<sup>26</sup> [ $Cu(D,L-2-aBut)_2$ ], *trans*-bis(L-2-aminobutyrate)copper(II)<sup>27</sup> [ $Cu(L-2-aBut)_2$ ], *cis*-bis(D-alaninato)copper(II)<sup>29</sup> [ $Cu(D-Ala)_2$ ], *trans*-Cu(Et<sub>2</sub>Gly)<sub>2</sub>,<sup>37</sup> *trans*-aquabis(L-*N,N*-dimethylvalinato)copper(II) hydrate<sup>32</sup> [ $Cu(L-Me_2Val)_2 \cdot 2H_2O$ ], *trans*-aquabis(L-*N,N*-diethylalaninato)copper(II)<sup>33</sup> [ $Cu(L-Et_2Ala)_2 \cdot 2H_2O$ ], *trans*-bis(D,L-alaninato)copper(II) monohydrate<sup>40</sup> [ $Cu(D,L-Ala)_2 \cdot H_2O$ ], *trans*-diaquabis(sarcosinato)copper(II)<sup>39</sup> [ $Cu(Sar)_2 \cdot 2H_2O$ ], *trans*-aquabis(L-*N,N*-dimethylalaninato)copper(II) hexahydrate<sup>34</sup> [ $Cu(L-Me_2Ala)_2 \cdot 7H_2O$ ], and *trans*-aquabis(*N*-*tert*-butyl-*N*-methylglycinato)-copper(II)<sup>36</sup> [ $Cu(tBuMeGly)_2 \cdot H_2O$ ]. The empirical parameters were systematically tested on the set of 12 additional copper(II) amino acid complexes, by modeling the crystal and molecular structures of seven anhydrous and five aqua copper(II) complexes: *trans*-bis(D,L-*N,N*-dimethylvalinato)-copper(II)<sup>24</sup> [ $Cu(D,L-Me_2Val)_2$ ], *trans*-bis(L-*N,N*-dimethylisoleucinato)copper(II)<sup>23</sup> [ $Cu(L-Me_2Ile)_2$ ], *trans*-bis(L-*N,N*-dipropylalaninato)copper(II)<sup>31</sup> [ $Cu(L-Pr_2Ala)_2$ ], *trans*-<sup>25</sup> and *cis*-<sup>30</sup> bis(L-alaninato)copper(II), [ $Cu(L-Ala)_2$ ], *trans*-bis(1-aminocyclopentanecarboxylato)copper(II)<sup>25</sup> [ $Cu(1-Acp)_2$ ], *trans*-bis( $\alpha$ -aminoisobutyrate)copper(II)<sup>28</sup> [ $Cu(\alpha-aiBut)_2$ ], *trans*-aquabis(L-*N,N*-dimethylisoleucinato)copper(II)<sup>35</sup> [ $Cu(L-Me_2Ile)_2 \cdot H_2O$ ], *trans*-aquabis(*N,N*-dimethylglycinato)copper(II) dihydrate<sup>38</sup> [ $Cu(Me_2Gly)_2 \cdot 3H_2O$ ], *trans*-aquabis(*N,N*-dimethylglycinato)copper(II)<sup>38</sup> [ $Cu(Me_2Gly)_2 \cdot H_2O$ ], *cis*-bis(glycinato)copper(II) hydrate<sup>41</sup> [ $Cu(Gly)_2 \cdot H_2O$ ], *cis*-aquabis(L-isoleucinato)copper(II)<sup>42</sup> [ $Cu(L-Ile)_2 \cdot H_2O$ ]. To ensure the planarity of the copper(II) coordination geometry for

Table 1. Potential Energy Parameter Set<sup>a,b</sup>

Morse Potential Parameters			
bond	$D_e$	$\alpha$	$b_0$
Cu-N	219.4140	2.2000	1.9900
N-C	52.4710	3.6000	1.4650
C-C	62.3610	4.0700	1.5150
C-H	101.6000	1.8000	1.0900
$O_W-H(O_W)$	200.0000	1.4360	0.9800
N-H	93.0000	2.5000	1.0100
$C_{pl}-O_{carbonyl}$	54.6840	3.4800	1.2300
C-C <sub>pl</sub>	114.1670	3.9500	1.5220
C <sub>pl</sub> -O	59.1680	2.7000	1.2900
Cu-O	85.7680	2.8500	1.9010
Valence Angle Potential Parameters			
valence angle	$k_\theta$	$\theta_0$	
Cu-N-H	55.0000	1.9106	
$H(O_W)-O_W-H(O_W)$	91.5390	1.9106	
Cu-N-C	240.0000	1.9106	
N-C-C	450.0000	1.9106	
N-C-H	356.0000	1.9106	
H-N-H	310.0000	1.9106	
H-C-H	276.8110	1.9106	
C-N-H	653.0000	1.9106	
H-C-C	304.1030	1.9106	
C-C-C	803.6020	1.9106	
C-N-C	185.0000	1.9106	
$C_{pl}-C-H$	471.1910	1.9106	
N-C-C <sub>pl</sub>	434.7020	1.9106	
C-C-C <sub>pl</sub>	235.0390	1.9106	
$O-C_{pl}-O_{carbonyl}$	717.4690	2.1640	
$C-C_{pl}-O_{carbonyl}$	383.8770	2.0940	
C-C <sub>pl</sub> -O	400.0000	2.0250	
$C_{pl}-O-Cu$	1100.0000	2.0070	
Torsion Potential Parameters			
torsion angle	$V_\varphi$	$n$	
C-C-C-N	9.5000	3.0000	
C-C-N-Cu	6.0500	3.0000	
Cu-O-C <sub>pl</sub> -C	5.6000	-4.0000	
O-C <sub>pl</sub> -C-N	0.7000	12.0000	
$C_{pl}-O-Cu-N$	4.3000	-4.0000	
O-Cu-N-C	0.0900	12.0000	
O-N-N-O	16.8000	-2.0000	
Out-of-Plane Torsion Potential Parameter			
out-of-plane torsion angle	$k_\chi$		
$O_{carbonyl}(C_{pl}-C-O)$	45.0000		
Lennard-Jones Potential Parameters			
atom	$A$	$B$	
H	80.0000	3.5810	
C	773.3199	9.7291	
N	4451.0765	119.5843	
O	1683.3682	73.8745	
$O_W$	793.3470	25.0000	
$O_{carbonyl}$	690.0000	40.3744	
Cu	210.0000	4.3919	
$C_{pl}$	310.0000	9.1000	
$H(O_W)$	0.0000	0.0000	
Charge Parameter			
atom	$q$		
$O_W$	-1.2698		
$H(O_W)$	0.0010		

<sup>a</sup> Uncommon symbols:  $C_{pl}$ , planar carbon atom;  $O_{carbonyl}$ , double-bonded oxygen atom,  $O_W$ , water oxygen. <sup>b</sup> Units are as follows:  $D_e$ , kcal mol<sup>-1</sup>;  $\alpha$ , Å<sup>-1</sup>;  $b_0$ , Å;  $k_\theta$ , kcal mol<sup>-1</sup> rad<sup>-2</sup>;  $\theta_0$ , rad;  $V_\varphi$ , kcal mol<sup>-1</sup>;  $A$ , (kcal mol<sup>-1</sup> Å<sup>12</sup>)<sup>1/2</sup>;  $B$ , (kcal mol<sup>-1</sup> Å<sup>6</sup>)<sup>1/2</sup>;  $q$ , electron units (therefore, the expression for electrostatic interactions has to be multiplied by 332.091 kcal mol<sup>-1</sup> Å in order to be in kcal mol<sup>-1</sup>).

anhydrous molecules in vacuo as obtained by quantum chemical calculations,<sup>58</sup> the parameters were optimized with

respect to the B3LYP valence angles around copper in three trans copper(II) chelates:<sup>58</sup>  $\text{Cu}(\text{L-Me}_2\text{Val})_2$ ,  $\text{Cu}(\text{L-Ala})_2$ , and  $\text{Cu}(\text{L-Leu})_2$ . They were then tested on the B3LYP calculated gas-phase structures of four aqua copper(II) glycinate complexes:<sup>59</sup> *cis*- $\text{Cu}(\text{Gly})_2 \cdot \text{H}_2\text{O}$ , *trans*- $\text{Cu}(\text{Me}_2\text{Gly})_2 \cdot 3\text{H}_2\text{O}$ , *trans*- $\text{Cu}(\text{Sar})_2 \cdot 2\text{H}_2\text{O}$ , and *trans*- $\text{Cu}(\text{tBuMeGly})_2 \cdot \text{H}_2\text{O}$

The empirical parameters were reoptimized and fitted with the aim to obtain a potential energy parameter set that could yield the best possible reproduction of experimental crystal structures and in vacuo B3LYP structures, regardless of whether the modeled systems were anhydrous or included interactions with water molecules. A problem that might arise during the parameter fitting process is that several combinations of the potential energy parameter set might yield the same reproduction results. A solution to this problem was sought by restricting the empirical parameter hyperspace with several specific conditions that the force field had to fulfill to be considered reliable. We used the same seven conditions as before,<sup>59</sup> plus an additional one (denoted condition 8 below). Specifically, the conditions were (1) to yield both trans and cis amino acid chelation to copper(II); (2) in  $\text{Cu}(\text{Sar})_2 \cdot 2\text{H}_2\text{O}$ , to allow for the movement of  $2\text{H}_2\text{O}$  from the axial position (as in the experimental crystal structure)<sup>39</sup> to the equatorial position (as in the equilibrium vacuum B3LYP structure)<sup>59</sup> accompanied by a conformational change<sup>59</sup> during in vacuo energy minimization; (3) to be able to simulate pronounced distortion from planarity of the chelate rings in aqua relative to anhydrous complexes; (4) to preserve the 2-fold crystallographic symmetry in the simulated crystal lattices of aquabis Cu(II) complexes with L-Me<sub>2</sub>Ala, L-Et<sub>2</sub>Ala, and tBuMeGly, with Cu(II) and O<sub>w</sub> on a 2-fold axis; (5) to retain the irregular square-planar copper(II) coordination geometry in the complexes that have such coordination in the crystal state; (6) to retain in vacuo distorted planar copper(II) coordination geometry<sup>58</sup> for anhydrous complexes; (7) to keep the positions of the water molecules as close to their experimental crystal and B3LYP vacuum positions as possible; and (8) to be able to reproduce the span of experimental intermolecular Cu—O<sub>carbonyl</sub> distances from 2.3 to 3.1 Å.

The final force field, named FFWa-SPCE (Table 1), met all eight special requirements and still yielded the geometry reproduction of the anhydrous and aqua copper(II) amino acid complexes in vacuo and in crystal comparable to that obtained by the force field FFW (see sections below). The empirical parameters of the bond-stretching, valence-angle-bending, torsion, out-of-plane-deformation, and Lennard-Jones potentials of the FFWa-SPCE force field are listed in Table 1. The charge parameters and fractional charge values assigned according to these parameters by the Lyngby-CFF program are given elsewhere.<sup>31,37,59</sup> The charge parameters for O<sub>w</sub> and H(O<sub>w</sub>) in Table 1 yielded fractional charges of  $-0.8476e$  and  $0.4238e$ , respectively, as assigned by the Lyngby-CFF program and were the same in all studied systems.

**Efficacy of the New Force Field.** To examine the efficacy of the new force field, the MM equilibrium geometries calculated in simulated crystalline surroundings and for isolated systems were compared with the experimental crystal

data<sup>21–42</sup> and the ab initio B3LYP-derived vacuum geometries,<sup>58,59</sup> respectively. The FFWa-SPCE results were compared with the results yielded by the FFW force field,<sup>37,38,59</sup> to examine the simulation ability of the new force field relative to that of FFW. The comparisons between the two force fields' results also indicate the validity of the MM model used. The suitability of FFWa-SPCE for simulations and predictions in aqueous solution was examined for solvated  $\text{Cu}(\text{Gly})_2$ , the only bis(amino acidato)copper(II) system for which, as mentioned in the Introduction, some experimental structural data in aqueous solution at room temperature were available from the literature.<sup>20</sup>

**MM Simulations in Crystal.** The experimental atomic coordinates and the unit cell lengths and angles were taken as the starting points for geometry optimization using the crystal simulator of the Lyngby-CFF program. Table 2 shows errors in reproducing the experimental internal coordinates and unit cell dimensions for each compound, total root-mean-square (rms) deviations between the experimental and theoretical values calculated for the anhydrous and aqua complexes separately, and the grand total rms values for all 25 compounds.

The FFWa-SPCE rms deviations between experimental and theoretical internal coordinates and unit cell dimensions are very much comparable to the values obtained with the FFW force field and discussed elsewhere.<sup>37,38,59</sup> In particular, using FFW, the total rms deviations for anhydrous complexes in the bond lengths, valence angles, torsion angles, and unit cell lengths are 0.018 Å, 2.2°, 4.6°, and 0.287 Å, respectively; for aqua complexes, the corresponding values are 0.016 Å, 2.3°, 6.1°, and 0.475 Å; and the grand total rms values for all 25 complexes are 0.017 Å, 2.2°, 5.3°, and 0.381 Å. The maximum difference between the experimental and theoretical unit cell angles is 9.6° by FFWa-SPCE and 8.7° by FFW [for  $\text{Cu}(\text{D,L-Ala})_2 \cdot \text{H}_2\text{O}$ ]. Experimental unit cell volumes are reproduced from  $-5.4\%$  to  $7.0\%$  by FFWa-SPCE and from  $-8.1\%$  to  $9.6\%$  by FFW.

FFWa-SPCE is capable of simulating the flexibility (plasticity) of the copper(II) coordination (Table S1, Supporting Information). Table S1 (Supporting Information) presents the mean values and standard deviations for the experimental and FFWa-SPCE crystal coordination polyhedron Cu—N and Cu—O bond lengths and angles around copper for all studied copper(II) amino acidates. The differences between the theoretical and experimental means are commonly within the standard deviations given in Table S1 (Supporting Information). The shapes of the coordination polyhedra are generally well reproduced by FFWa-SPCE as well as by FFW.<sup>59</sup> FFWa-SPCE maintains the planarity of the copper(II) coordination polyhedron in the crystal (as well as in vacuo) for all molecules whose amino acid donor atoms form an irregular square-planar configuration around the copper(II) in the experimental crystal lattice.

The intermolecular axial copper—carbonyl-oxygen distances are experimentally in the range from 2.312 to 3.116 Å (Table S2, Supporting Information). The new force field manages to cover a greater span of the particular distances (from 2.376 to 2.877 Å; Table S2, Supporting Information) than the force field FFW (from 2.519 to 2.855 Å; Table S2,



**Table 2.** Comparison of Experimental and FFWa-SPCE Crystal Structures in Terms of the Root-Mean-Square Deviations (rms) in Internal Coordinates<sup>a</sup> and Unit Cell Constants (*a*, *b*, and *c*, in Å) and Differences,  $\Delta$ , between Experimental and Theoretical Unit Cell Angles ( $\alpha$ ,  $\beta$ , and  $\gamma$ , in deg) and Volumes (*V*)

compound	rms( $\Delta b$ )	rms( $\Delta\theta$ )	rms( $\Delta\varphi$ )	rms( $\Delta a, \Delta b, \Delta c$ )	$\Delta\alpha, \Delta\beta, \Delta\gamma$	100 $\Delta V/V_{\text{exp}}$
Cu(L-Me <sub>2</sub> Val) <sub>2</sub>	0.015	2.4	2.9	0.525	0.0, 0.0, 0.0	-1.4
<i>trans</i> -Cu(L-Ala) <sub>2</sub>	0.017	2.7	4.1	0.207	0.0, 3.7, 0.0	-2.3
Cu(L-Leu) <sub>2</sub>	0.016	2.2	4.2	0.263	0.0, -1.1, 0.0	-0.4
Cu(D,L-2-aBut) <sub>2</sub>	0.015	1.7	4.2	0.171	0.0, -0.7, 0.0	-4.6
Cu(1-Acpc) <sub>2</sub>	0.010	1.7	1.6	0.139	0.0, 4.6, 0.0	-2.4
Cu(D,L-Et <sub>2</sub> Ala) <sub>2</sub>	0.030	1.9	3.4	0.240	4.2, 1.3, -3.5	2.7
Cu(D,L-Me <sub>2</sub> Val) <sub>2</sub>	0.010	1.5	0.9	0.109	0.0, 1.1, 0.0	1.0
Cu(L-2-aBut) <sub>2</sub>	0.017	2.2	4.9	0.254	0.0, 1.2, 0.0	-3.2
Cu( $\alpha$ -aiBut) <sub>2</sub>	0.015	2.2	3.1	0.151	0.0, -0.7, 0.0	0.5
Cu(L-Me <sub>2</sub> Ile) <sub>2</sub>	0.020	2.7	4.7	0.479	0.0, 0.5, 0.0	-0.5
Cu(L-Pr <sub>2</sub> Ala) <sub>2</sub>	0.018	1.7	3.4	0.254	0.0, -0.2, 0.0	-5.4
Cu(D-Ala) <sub>2</sub>	0.024	1.8	5.1	0.209	0.0, 0.0, 0.0	-4.4
<i>cis</i> -Cu(L-Ala) <sub>2</sub>	0.009	1.9	5.7	0.207	0.0, 0.0, 0.0	-4.1
Cu(Et <sub>2</sub> Gly) <sub>2</sub>	0.018	2.5	3.6	0.041	0.0, 0.0, 0.0	-0.1
<i>total</i>	0.018	2.1	3.8	0.264		
Cu(L-Me <sub>2</sub> Val) <sub>2</sub> ·2H <sub>2</sub> O	0.010	1.7	3.5	0.816	1.7, 2.5, 4.1	2.6
Cu(Sar) <sub>2</sub> ·2H <sub>2</sub> O	0.018	1.2	5.8	0.640	0.0, -2.7, 0.0	2.8
Cu(L-Et <sub>2</sub> Ala) <sub>2</sub> ·H <sub>2</sub> O	0.019	1.7	5.3	0.268	0.0, 0.0, 0.0	1.3
Cu(tBuMeGly) <sub>2</sub> ·H <sub>2</sub> O	0.021	3.2	5.9	0.101	0.0, 0.0, 0.0	1.6
Cu(L-Me <sub>2</sub> Ile) <sub>2</sub> ·H <sub>2</sub> O	0.016	2.1	4.5	0.092	0.0, 0.0, 0.0	1.1
Cu(D,L-Ala) <sub>2</sub> ·H <sub>2</sub> O	0.023	2.5	8.5	0.769	0.0, 9.6, 0.0	4.4
Cu(L-Me <sub>2</sub> Ala) <sub>2</sub> ·7H <sub>2</sub> O	0.008	2.0	1.7	0.524	0.0, 2.7, 0.0	7.0
Cu(Gly) <sub>2</sub> ·H <sub>2</sub> O	0.018	1.3	14.2	0.473	0.0, 0.0, 0.0	3.8
Cu(L-Ile) <sub>2</sub> ·H <sub>2</sub> O	0.013	3.2	6.7	0.123	0.0, 0.0, 0.0	-2.6
Cu(Me <sub>2</sub> Gly) <sub>2</sub> ·3H <sub>2</sub> O	0.011	2.1	3.3	0.179	0.0, 0.0, 0.0	6.0
Cu(Me <sub>2</sub> Gly) <sub>2</sub> ·H <sub>2</sub> O	0.012	2.2	2.8	0.197	0.0, 0.0, 0.0	1.1
<i>total</i>	0.016	2.2	6.4	0.461		
<b>grand total</b>	<b>0.017</b>	<b>2.2</b>	<b>5.0</b>	<b>0.364</b>		

<sup>a</sup> Internal coordinates: bond lengths, *b* (in Å), valence angles,  $\theta$  (in deg), torsion angles  $\varphi$  (in deg). Hydrogen atoms were not taken into account.

Supporting Information), and hence, FFWa-SPCE copes quite well with the eighth special condition used in the force field parameterization. Both force fields overestimate the means of the copper—axial-water-oxygen-atom distances by 0.2 Å (Table S3, Supporting Information). This result is due to the force field parameterization procedure, that is, the best possible reproduction obtained by taking all special force field parameterization requirements for a reliable force field into the consideration.

Good overall reproduction of the experimental crystal and molecular structures confirms that FFWa-SPCE is reliable; specifically, it accurately reproduces the crystal lattice effects, and the van der Waals and hydrogen-bonding intermolecular interactions are properly modeled.

**MM Simulations in Vacuo.** A very good match obtained between vacuum quantum chemical B3LYP structures<sup>58</sup> and MM minimum geometries calculated by the two force fields, FFW and FFWa-SPCE, for three anhydrous copper(II) amino acid complexes is shown in Figure 1. FFWa-SPCE yielded very much the same reproduction of the B3LYP structures as FFW (discussed elsewhere<sup>59</sup>).

For the four copper(II) bis-glycinato systems containing from one to four water molecules (Figure 2), the match between the MM and B3LYP structures<sup>59</sup> is not as good as for the anhydrous complexes (as the aqua complexes are generally more difficult to model than the anhydrous com-

plexes),<sup>59</sup> but it is still acceptable. Both force fields similarly reproduce molecular structures of the copper(II) glycinato complexes, although they yield different positions for the water molecules (Figure 2). The new force field overestimates the B3LYP Cu—O<sub>w</sub> axial distance by 0.03 and 0.27 Å in *cis*-Cu(Gly)<sub>2</sub>·H<sub>2</sub>O and *trans*-Cu(Me<sub>2</sub>Gly)<sub>2</sub>·3H<sub>2</sub>O, respectively. The B3LYP and FFWa-SPCE-calculated hydrogen-bond distances between O<sub>w</sub> and carboxylato oxygen atoms also differ slightly, from -0.14 Å to 0.15 Å. The ab initio O...O<sub>w</sub> and N...O<sub>w</sub> hydrogen-bond distances amount, respectively, to 2.76 and 3.05 Å in *cis*-Cu(Gly)<sub>2</sub>·H<sub>2</sub>O and 2.72 and 2.89 Å in *trans*-Cu(Sar)<sub>2</sub>·2H<sub>2</sub>O.<sup>59</sup> FFWa-SPCE overestimates the corresponding distances by 0.12 and 0.35 Å in the *cis* complex and by 0.10 Å and 0.63 Å in the *trans* complex, still yielding values generally accepted to count as hydrogen bonds.

**MD Simulations of Cu(Gly)<sub>2</sub> in Aqueous Solution at Room Temperature.** MD simulations were performed using the new force field FFWa-SPCE. The out-of-plane deformation angle,  $\chi$  (improper dihedral angle), is differently defined in the Lyngy-CFF program [as the angle between the plane defined by (C, C<sub>pl</sub>, O) and O<sub>carbonyl</sub>] than in Gromacs [as the angle between two planes defined by (C, C<sub>pl</sub>, O) and by (C, O<sub>carbonyl</sub>, O)]. To get the same equilibrium geometries in vacuo by the two programs, the empirical parameter of the

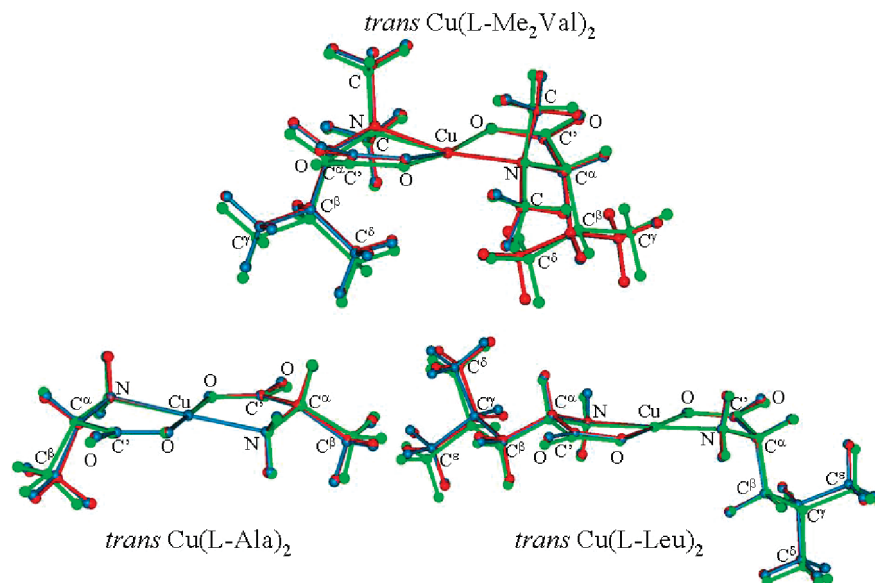


**Figure 1.** Superposition of in vacuo equilibrium geometries of three anhydrous copper(II) amino acid complexes: structures obtained using B3LYP (green), MM FFW (red), and FFWa-SPCE (blue).

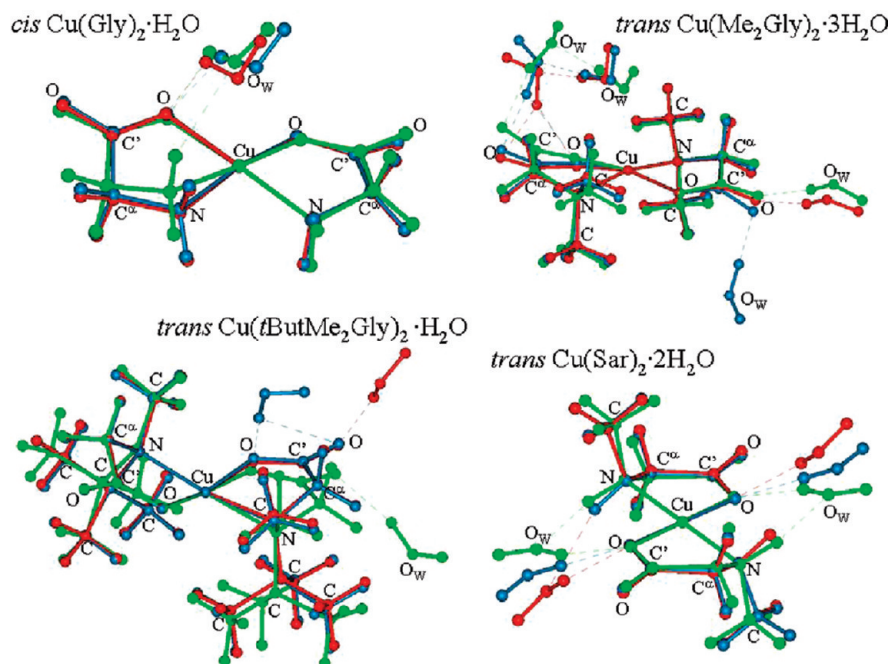


**Figure 2.** Superposition of the equilibrium geometries of four isolated aquabis glycinate copper(II) systems: structures obtained using B3LYP (green), MM FFW (red), and FFWa-SPCE (blue).

out-of-plane deformation potential  $V(\chi)$  in eq 1 was adjusted to  $k_\chi = 99.5 \text{ kcal mol}^{-1} \text{ rad}^{-2}$  for use in Gromacs.

The ability of the FFWa-SPCE force field to predict structural properties in aqueous solution was examined by simulating solvated *cis*- and *trans*-Cu(Gly)<sub>2</sub> and by comparing the theoretical MD results with experimental data<sup>20</sup> obtained by X-ray absorption spectroscopy. Table 3 presents selected experimental structural coordinates (the technique could not distinguish one isomer from the other), along with the corresponding values of the average MD structures, as well as the means and standard deviations of the coordinate values obtained during 20 ns of MD simulations at room temperature, separately for the *trans* and *cis* isomers. Table 3 also includes the results obtained by quantum chemical

PCM calculations at the B3LYP/LanL2DZ{D95v+(d)} level of theory. The MD copper—water-oxygen-atom distances in the first and second coordination spheres (or second hydration shell) in Table 3 were obtained from the Cu—O<sub>w</sub> radial distribution functions (Figure 3).

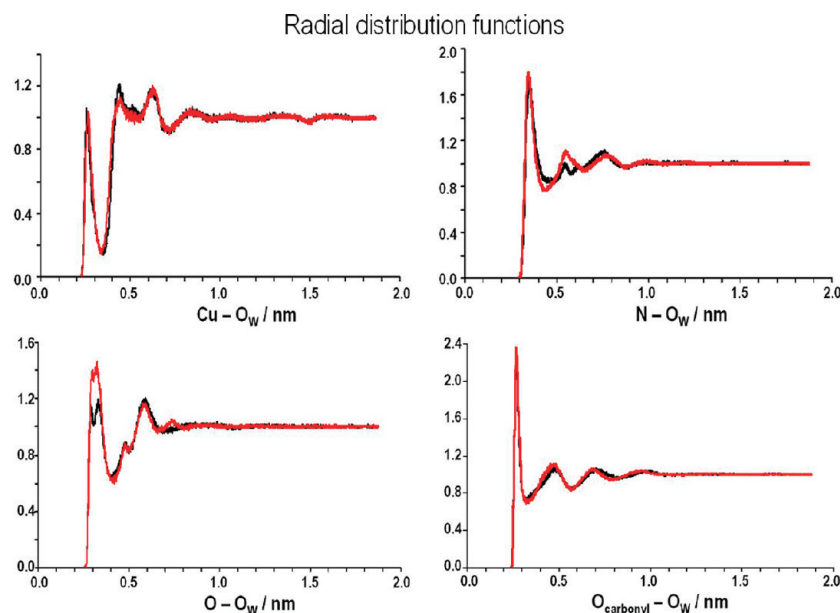
The deviations between the theoretical means and the experimental values of the bond distances and angles are within the theoretical and experimental error values (Table 3). This statement also applies to the valence angles around copper(II), although their values suggest the distortion of the copper(II) coordination geometry from planarity for the solvated complex during MD simulations. The distribution functions for the valence angles around copper(II) estimated from the MD simulation data revealed the most frequent



**Table 3.** Selected Structural Coordinates of Cu(Gly)<sub>2</sub> in Aqueous Solution at Room Temperature As Obtained from X-ray Absorption Studies<sup>a</sup> and Estimated from 20 ns of MD Simulations and by the PCM Method Separately for *trans*- and *cis*-Cu(Gly)<sub>2</sub><sup>b</sup>

coordinate	X-ray absorption <sup>a</sup>		MD (FFWa-SPCE force field)				PCM	
			average structure					
	value	variance	trans <sup>c</sup>	cis <sup>c</sup>	trans	cis	trans	cis
Cu—N	1.99	0.004	2.00 (1)	2.00 (2)	1.98	1.97	2.02	2.03
Cu—O	1.95	0.006	1.93 (2)	1.92 (2)	1.91	1.92	1.96	1.96
Cu⋯C <sup>α</sup>	2.84	0.020	2.83 (3)	2.82 (3)	2.79	2.79	2.88	2.88
Cu⋯C′	2.79	0.003	2.73 (3)	2.73 (3)	2.69	2.71	2.79	2.79
C′=O	1.24	0.006	1.23 (2)	1.23 (2)	1.20	1.21	1.24	1.24
N—Cu—N			167 (7)		179.7		179.5	
N—Cu—O	179	36		169 (7)		175.3		177.4
O—Cu—O			167 (7)		179.7		179.8	
Cu—C′=O	168	36	161 (3)	161 (2)	163.0	163.2	163.0	162.9
Cu⋯O <sub>W,ax</sub>	2.40 (6)	0.03 (1)	2.6	2.6				
Cu⋯O <sub>W,s</sub>	3.3 (2)	0.06 (3)	3.5	3.4				

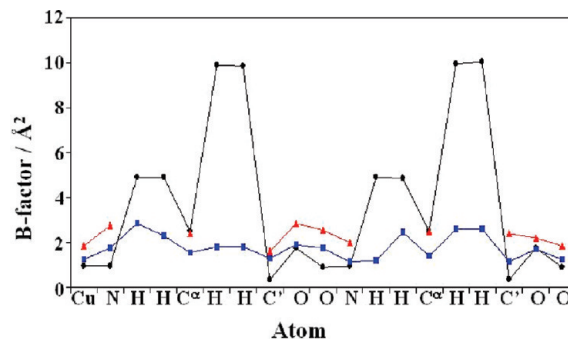
<sup>a</sup> Reference 20. <sup>b</sup> Bond distances are in Å, and bond angles are in deg. Bond and angle variances are in Å<sup>2</sup> and deg<sup>2</sup>, respectively. Standard deviations are in parentheses. The O<sub>W,ax</sub> and O<sub>W,s</sub> denote the water oxygen atoms from the first and second coordination spheres, respectively. <sup>c</sup> Means and standard deviations calculated from the values attained in 20-ns trajectories.

**Figure 3.** Radial distribution functions for solvated *trans*-Cu(Gly)<sub>2</sub> (black) and *cis*-Cu(Gly)<sub>2</sub> (red) determined during 20 ns of MD simulation at room temperature.

values to be 172° and 171° for the N–Cu–N and O–Cu–O angles, respectively, in *trans*-Cu(Gly)<sub>2</sub> and 173° for the N–Cu–O angles in *cis*-Cu(Gly)<sub>2</sub>.

Although the average structures obtained from the MD simulations might not necessarily represent physically reasonable structures, their structural coordinates (Table 3) are in very good agreement with the experimental values (within experimental errors) and the PCM coordinates.

The *B* factor, which is estimated from the rms fluctuations of the atoms, was calculated and compared with available experimental values from the X-ray diffraction measurements of *cis*-Cu(Gly)<sub>2</sub>·H<sub>2</sub>O at room temperature<sup>41</sup> and 173 K<sup>43</sup> (Figure 4). The calculated *B* factors, which indicate the atom motions in aqueous solution at room temperature, follow the general pattern of the experimental *B* factors for heavy atoms with a few exceptions, namely, the hydrogen-atom fluctuations are calculated as more pronounced in solution at 300 K under the influence of solvent–solute interactions than as measured in

**Figure 4.** *B* factors for the atoms of *cis*-Cu(Gly)<sub>2</sub> calculated from the MD simulation (black) and from experimental X-ray crystal structures of *cis*-Cu(Gly)<sub>2</sub>·H<sub>2</sub>O measured at room temperature (red) and at 173 K (blue) as reported in refs 41 and 43, respectively.

the 173 K crystal structure (Figure 4). Apparently, the MD simulations reproduced the molecular motion reasonably well.

**Table 4.** MD Average Values of Energy Contributions and Corresponding rms Deviations (in Parentheses) Calculated from the Values Attained during 20 ns of MD Simulations at Room Temperature Separately for the *trans*- and *cis*-Cu(Gly)<sub>2</sub>·2159H<sub>2</sub>O Systems

	energy (kJ mol <sup>-1</sup> )			
	trans		cis	
potential energy	-101604.0	(244.9)	-101609.0	(246.4)
kinetic energy	16309.3	(148.0)	16311.1	(148.2)
total energy	-85294.8	(196.5)	-85298.2	(198.9)
Cu(Gly) <sub>2</sub> Intramolecular Contributions				
<i>V</i> ( <i>b</i> )	26.3	(8.4)	27.7	(8.7)
<i>V</i> ( <i>θ</i> )	37.1	(9.3)	34.9	(9.0)
<i>V</i> ( <i>φ</i> )	46.7	(5.2)	45.9	(5.2)
<i>V</i> ( <i>χ</i> )	2.0	(1.7)	2.0	(1.7)
<i>V</i> <sub>Coulomb,NB</sub>	-1516.1	(19.6)	-1388.8	(14.8)
<i>V</i> <sub>Coulomb,1-3</sub>	2299.1	(19.1)	2290.5	(15.9)
<i>V</i> <sub>LJ</sub>	-21.0	(2.0)	-19.9	(2.8)
total	874.1		992.3	
Intermolecular Cu(Gly) <sub>2</sub> ·H <sub>2</sub> O Contributions				
<i>V</i> <sub>Coulomb</sub> (short-range)	-415.3	(43.6)	-587.8	(51.2)
<i>V</i> <sub>Coulomb</sub> (long-range)	-35.4	(29.5)	-72.0	(32.6)
<i>V</i> <sub>LJ</sub> (short-range)	-114.6	(15.9)	-114.0	(16.2)
<i>V</i> <sub>LJ</sub> (long-range)	-6.3	(0.2)	-6.3	(0.2)
Intermolecular H <sub>2</sub> O·H <sub>2</sub> O Contributions				
<i>V</i> <sub>Coulomb</sub> (short-range)	-117708.0	(414.5)	-117588.0	(416.4)
<i>V</i> <sub>Coulomb</sub> (long-range)	-3436.1	(230.0)	-3467.4	(228.5)
<i>V</i> <sub>LJ</sub> (short-range)	19522.0	(256.3)	19518.3	(257.3)
<i>V</i> <sub>LJ</sub> (long-range)	-284.4	(1.1)	-284.6	(1.1)

Table 4 presents average values and corresponding rms deviations of energy contributions for the *trans*- and *cis*-Cu(Gly)<sub>2</sub>·2159H<sub>2</sub>O systems calculated during 20 ns of MD simulations. Although the intramolecular potential energy contribution was lower for the *trans* isomer than for the *cis* isomer, the *cis* isomer had more favorable electrostatic interactions with the water molecules. Different interactions between the *trans* and *cis* conformations with the water molecules [also noticeable in the different organization structures of the water molecules around the isomers in Figure 3 from the radial distribution functions calculated for the distances between O<sub>W</sub> and atoms of Cu(Gly)<sub>2</sub> that form hydrogen bonds with water molecules] influenced the water–water interactions as well. As a result, the two systems had similar total energies, with the average total energy of the solvated *cis*-isomer system being 3 kJ mol<sup>-1</sup> lower than that of the solvated *trans*-isomer system (Table 4). The MD prediction is in line with the quantum chemical PCM energy estimations for the two isomers in approximate aqueous medium at 300 K, which predicted a small energy difference of 4.96 kJ mol<sup>-1</sup> in favor of *trans*-Cu(Gly)<sub>2</sub>. Moreover, recent EPR measurements of Cu(Gly)<sub>2</sub> in glycerol/water solution confirmed the simultaneous presence of both isomers at room temperature.<sup>19</sup>

**Cis–Trans Isomerization of Cu(Gly)<sub>2</sub> in Aqueous Solution at 300 K.** Table 5 lists the energy differences between the *cis* and *trans* minima and the TS structure of Cu(Gly)<sub>2</sub> calculated at the B3LYP/LanL2DZ{D95v+(d)} level of theory in the gas phase and in water medium at room temperature. The stationary points in the gas phase were calculated and compared with the geometries and energies obtained at the higher level of theory [denoted as G3(MP2)-B3<sub>LanL2DZ</sub> elsewhere]<sup>64</sup> to verify the basis set and the method used. The B3LYP/LanL2DZ{D95v+(d)} gas-phase potential

**Table 5.** Potential Energy (Δ*V*) and Gibbs Free Energy (Δ*G*) Barriers for the Isomerization Reaction of Cu(Gly)<sub>2</sub> in the Gas Phase and in Aqueous Solution at 300 K Calculated at the B3LYP/LanL2DZ{D95v+(d)} Level of Theory and Reaction Rates Calculated from Eqs 2a and 2b

	gas phase	aqueous solution
Energy Difference (kJ mol <sup>-1</sup> )		
Δ <i>V</i> <sub>TS→cis</sub>	28.95	70.10
Δ <i>V</i> <sub>TS→trans</sub>	85.69	75.06
Δ <i>G</i> <sub>TS→cis</sub>	26.26	63.67
Δ <i>G</i> <sub>TS→trans</sub>	81.92	69.47
Reaction Rate (s <sup>-1</sup> )		
<i>k</i> <sub>cis→trans</sub>	1.7 × 10 <sup>8</sup>	51.3
<i>k</i> <sub>trans→cis</sub>	3.4 × 10 <sup>-2</sup>	5.0

energy values differ by 1 kcal mol<sup>-1</sup> from the higher theory's values,<sup>64</sup> yielding the same energy difference value of 56.74 kJ mol<sup>-1</sup> between the *cis* and *trans* minima. The geometries of the stationary points derived at the lower and higher levels of theory are almost the same, as the maximum differences between their internal coordinates are up to 0.015 Å in bond lengths (Cu–N), 3.7° in valence angles (N–C<sup>α</sup>–H), and 2.9° in torsion angles (C'–C<sup>α</sup>–N–Cu).

The TS geometries obtained in the gas phase and in solution were additionally fully optimized in water medium. Interestingly, in both instances initial guess of the orbital energies directed the optimization to the *cis* final structure. Nevertheless, with a different choice of initial orbital energies (by using the Vshift option under the G03 SCF keyword), the optimization of the TS structure in aqueous medium ended in *trans* structure, as would be expected from the isomer energy estimations that the *trans* isomer had lower energy than the *cis* isomer (Table 5).

Compared to the gas-phase results, the PCM calculations in aqueous solution revealed a slightly lower energy differ-

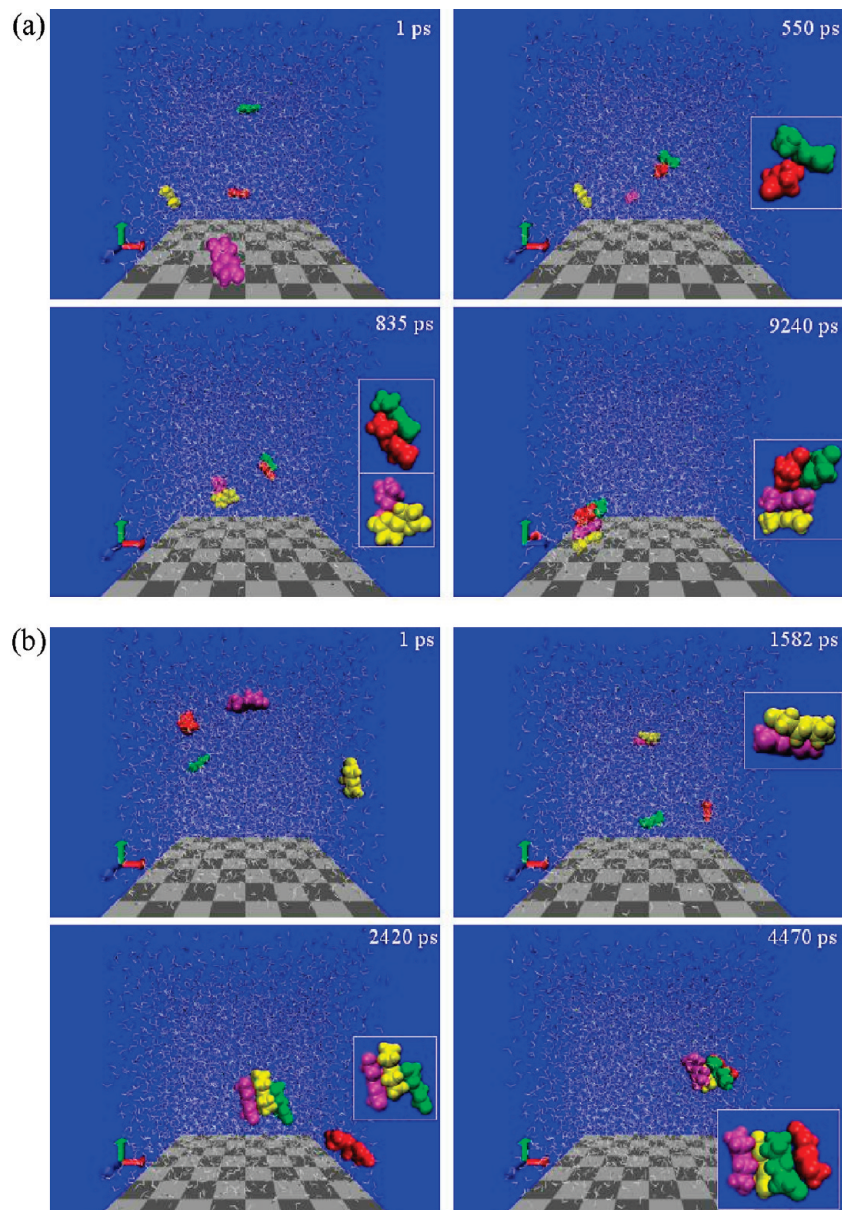


**Figure 5.** System of  $4\text{Cu}(\text{Gly})_2 \cdot 5457\text{H}_2\text{O}$  depicted at indicated times in MD simulations: (a) four trans isomers and (b) four cis isomers colored red, green, yellow, and magenta, with water molecules in white. The figure was prepared using the VMD program.<sup>102</sup>

**Table 6.** Aggregation Times (ps) of Four Solvated  $\text{Cu}(\text{Gly})_2$  Molecules during MD Simulations for Four Studied Systems Containing Four *trans*- $\text{Cu}(\text{Gly})_2$  Molecules, Four *cis*- $\text{Cu}(\text{Gly})_2$  Molecules, and Two *trans*- $\text{Cu}(\text{Gly})_2$  and Two *cis*- $\text{Cu}(\text{Gly})_2$  Molecules Having Different Initial Positions

$\text{Cu}(\text{Gly})_2$	dimer	trimer	tetramer
four trans	550, 885		9240
four cis	1582	2420	4470
two trans, two cis	125 (trans–trans)	1465 (cis–trans–trans)	12045 (cis–trans–trans–cis)
two trans, two cis	580 (cis–trans)	1615 (cis–trans–cis)	4605 (cis–trans–cis–trans)

ence between the trans isomer and the TS structure, but a considerably larger energy difference between the cis isomer and the TS structure (Table 5), resulting in a dramatic lowering of the potential energy difference between the trans and cis conformations.

This result raised the following question: If the energy difference between the cis and trans isomers is considerably

lower in aqueous solution than in the gas phase, as obtained by both MD and PCM calculations, why could a cis–trans interconversion of  $\text{Cu}(\text{Gly})_2$  not be obtained during the MD simulations? To find at least a qualitative answer to this question, we calculated the reaction rate constants for the isomerization reaction in aqueous solution and in the vacuum from eqs 2a and 2b (Table 5) and compared them with the



gas-phase rate constants determined by variational transition state theory including quantum effects such as tunneling and corner cutting.<sup>64</sup> The gas-phase calculations<sup>64</sup> showed that, at room temperature, the cis isomer spontaneously transforms into the trans isomer without breaking bonds, with reaction rate constants  $k_{\text{cis} \rightarrow \text{trans}}$  and  $k_{\text{trans} \rightarrow \text{cis}}$  equal to  $2.1 \times 10^6$  and  $2.7 \times 10^{-4} \text{ s}^{-1}$ , respectively. Hence, the gas-phase reaction rates calculated from the standard transition state theory (Table 5) are 2 orders of magnitude higher than the reaction rate constants obtained by more precise variational transition state theory. A contribution of 1 order of magnitude is caused by the difference between the high-level and low-level potential energy values of  $1 \text{ kcal mol}^{-1}$  (yielding 5.4 times larger rate constant values). Because the tunneling effect was calculated to be negligible at 300 K,<sup>64</sup> an additional contribution to the difference in the gas-phase rates should be due to a variational effect.<sup>98</sup> As the reaction rate constants were obtained using information only at the stationary points and assuming that the transmission factor was equal to unity, they can be considered as zeroth-order approximations of the actual rate constants. If we assume the same order-of-magnitude error for the calculation of the reaction rate values in aqueous solution (Table 5), then the interconversion between the cis and trans isomers in aqueous solution should be on the order from milliseconds to seconds, and this result is in accord with our not observing the isomerization during the MD simulations of 20 ns. Whether the assumption is correct remains to be examined by MD calculations of the free energy profile and activation free energy for the intramolecular cis–trans interconversion of  $\text{Cu}(\text{Gly})_2$  in aqueous solution in forthcoming studies. It would also be challenging to explore the possibility of cis–trans isomerization by an intermolecular process through a chelate ring-opening and bond-breaking and -forming mechanism. It would be appealing to probe the force field for creating a reactive force field (by adding new potential energy terms, and further reparameterization) to calculate a reactive potential energy surface and for proper configuration sampling in solution within, for example, an empirical valence bond (EVB) approach,<sup>99–101</sup> which uses classical MM force fields to model reactant and product configurations and can accurately describe reactive potential energy surfaces.

**Twenty-Nanosecond MD Simulations of the  $4\text{Cu}(\text{Gly})_2 \cdot 5457\text{H}_2\text{O}$  System.** The predictive properties of the FFWa-SPCE force field were examined on a system of four solvated  $\text{Cu}(\text{Gly})_2$  molecules in aqueous solution at room temperature. The MD trajectories were collected for systems containing four trans and four cis isomers (Figure 5). Interesting results were obtained as, after some time, the  $\text{Cu}(\text{Gly})_2$  complexes started to aggregate (Figure 5). The trans isomers formed two dimers that eventually aggregated to a tetramer. The cis isomers aggregated differently, from a dimer to a trimer to a tetramer. Two additional aggregation patterns were obtained for systems containing two trans and two cis isomers by taking different initial positions (Table 6). Although the aggregation patterns were different, these four MD trajectories offered some regularity. Interestingly, it was observed that, if a trans–trans dimer formed first, the aggregation to a tetramer required a longer time than if a

cis isomer formed the initial dimer (Table 6). The average total MD energy of the solvated trans tetramer system was lower than those of the cis tetramer system and the mixed two trans, two cis tetramer by 24 and 12  $\text{kJ mol}^{-1}$ , respectively.

The predicted results can be related to the experimental observations. Specifically, in the solid state, *trans*- $\text{Cu}(\text{Gly})_2$  is thermodynamically more stable than the cis isomer.<sup>103</sup> However, aqua *cis*- $\text{Cu}(\text{Gly})_2$  is the form that crystallizes upon slow evaporation of the aqueous solution at room temperature.<sup>41,43</sup> Thus, the MD-predicted aggregation results suggest that the crystallization process of  $\text{Cu}(\text{Gly})_2$  is a more kinetically than thermodynamically driven course of action.

## Conclusions

The new force field parameterization, as a continuation of our previous work on molecular modeling of copper(II) complexes with aliphatic  $\alpha$ -amino acids and their *N*-alkyl derivatives in the vacuum and simulated crystal surroundings,<sup>37,38,59</sup> enables the prediction of structural properties in aqueous solution as well. Specifically, the time-average bond distances and angles of  $\text{Cu}(\text{Gly})_2$  obtained during MD simulations in aqueous solution at room temperature with the new FFWa-SPCE force field are in good agreement with the experimental data obtained by X-ray absorption spectroscopy<sup>20</sup> and quantum chemical PCM calculations.

The quantum chemical PCM energy estimations of the trans and cis minima and TS structure of  $\text{Cu}(\text{Gly})_2$  in approximate water medium revealed a pronounced lowering of the energy difference between the two minima and an increase in the energy difference between the cis conformer and the TS structure with respect to the gas phase (Table 5). The MD-based estimations suggest that the decrease in energy difference was due to more favorable electrostatic interactions of the cis than the trans isomer with the water molecules. A small energy difference between the two solvated isomer systems is also predicted by the MD simulations and can be confirmed by experimental observations<sup>19</sup> that the trans and cis conformers of  $\text{Cu}(\text{Gly})_2$  are simultaneously present in aqueous solution at room temperature.

The use of the same set of relatively simple analytical functions with carefully selected empirical parameters for MM calculations in vacuo and in crystal, as well as MD simulations in aqueous solution, can provide structural and energetic information about bis(amino acidato)copper(II) compounds in these environments. Furthermore, the study can assist in understanding the self-association of the complexes in solution and identifying the formation of a nucleus of crystallization.

**Acknowledgment.** This work was supported by the Croatian Ministry of Science, Education and Sports (Project Grant 022-0222148-2822). We thank Dr Sanja Tomić (Ruđer Bošković Institute, Zagreb, Croatia) for encouragement and guidelines concerning the MD simulations and for critical reading and editing of the manuscript.

**Supporting Information Available:** Listing of means and standard deviations of the experimental and FFWa-SPCE

crystal bond lengths and angles of the copper(II) polyhedra in 14 anhydrous and 11 aqua copper(II) amino acidates (Table S1), reproduction of experimental in-crystal axial intermolecular  $\text{Cu} \cdots \text{O}_{\text{carbonyl}}$  distances (Table S2), and  $\text{Cu} \cdots \text{O}_{\text{W}}$  distances (Table S3) in 8 anhydrous and 11 aqua copper(II) amino acidates obtained using the FFW and FFWa-SPCE force fields, respectively. This material is available free of charge via the Internet at <http://pubs.acs.org/>.

## References

- (1) *Molecular Biology and Toxicology of Metals*; Zalups, R. K.; Koropatnick, J., Eds.; Taylor & Francis: London, 2000.
- (2) DiDonato, M.; Sarkar, B. *Biochem. Biophys. Acta* **1997**, *1360*, 3–16.
- (3) Deschamps, P.; Kulkarni, P. P.; Gautam-Basak, M.; Sarkar, B. *Coord. Chem. Rev.* **2005**, *249*, 895–909.
- (4) Kodama, H.; Fujisawa, C. *Metallomics* **2009**, *1*, 42–52.
- (5) Gaetke, L. M.; Chow, C. K. *Toxicology* **2003**, *189*, 147–163.
- (6) *Copper, Environmental Health Criteria 200*; International Programme on Chemical Safety (IPCS), World Health Organization: Geneva, Switzerland, 1998; available at <http://www.inchem.org/documents/ehc/ehc/ehc200.htm> (accessed Feb 28, 2008).
- (7) Dokmanić, I.; Šikić, M.; Tomić, S. *Acta Crystallogr.* **2008**, *D64*, 257–263.
- (8) Farkas, E.; Sóvágó, I. *Amino Acids, Pept. Proteins* **2007**, *36*, 287–345.
- (9) Szabó-Plánka, T.; Rockenbauer, A.; Korecz, L.; Nagy, D. *Polyhedron* **2000**, *19*, 1123–1131.
- (10) Szabó-Plánka, T.; Rockenbauer, A.; Korecz, L. *Polyhedron* **1999**, *18*, 1969–1974.
- (11) Szilágyi, I.; Labádi, I.; Hernadi, K.; Pálkó, I.; Nagy, N. V.; Korecz, L.; Rockenbauer, A.; Kele, Z.; Kiss, T. *J. Inorg. Biochem.* **2005**, *99*, 1619–1629.
- (12) Altun, Y.; Köseoğlu, F. *J. Solution Chem.* **2005**, *34*, 213–231.
- (13) Branica, G.; Paulić, N.; Grgas, B.; Omanović, D. *Chem. Speciation Bioavailability* **1999**, *11*, 125–134.
- (14) Mirosavljević, K.; Sabolović, J.; Noethig-Laslo, V. *Eur. J. Inorg. Chem.* **2004**, 3930–3937.
- (15) Sabolović, J.; Noethig-Laslo, V. *Cell. Mol. Biol. Lett.* **2002**, *7*, 151–153.
- (16) Goodman, B. A.; McPhail, D. B. *J. Chem. Soc., Dalton Trans.* **1985**, 1717–1718.
- (17) Goodman, B. A.; McPhail, D. B.; Powell, H. K. J. *J. Chem. Soc., Dalton Trans.* **1981**, 822–827.
- (18) Noethig-Laslo, V.; Paulić, N. *J. Chem. Soc., Dalton Trans.* **1992**, 2045–2047.
- (19) Pezzato, M.; Della Lunga, G.; Baratto, M. C.; Pogni, R.; Basosi, R. *Magn. Reson. Chem.* **2007**, *45*, 846–849.
- (20) D'Angelo, P.; Bottari, E.; Festa, M. R.; Nolting, H.-F.; Pavel, N. V. *J. Phys. Chem. B* **1998**, *102*, 3114–3122.
- (21) Kaitner, B.; Kamenar, B.; Paulić, N.; Raos, N.; Simeon, V. *J. Coord. Chem.* **1987**, *15*, 373–381.
- (22) Kaitner, B.; Ferguson, G.; Paulić, N.; Raos, N. *J. Coord. Chem.* **1992**, *26*, 105–115.
- (23) Kaitner, B.; Paulić, N.; Raos, N. *J. Coord. Chem.* **1991**, *22*, 269–279.
- (24) Kaitner, B.; Meštrović, E.; Paulić, N.; Sabolović, J.; Raos, N. *J. Coord. Chem.* **1995**, *36*, 117–124.
- (25) Hitchman, M. A.; Kwan, L.; Engelhardt, L. M.; White, A. H. *J. Chem. Soc., Dalton Trans.* **1987**, 457–465.
- (26) Fawcett, T. G.; Ushay, M.; Rose, J. P.; Lalancette, R. A.; Potenza, J. A.; Schugar, H. J. *Inorg. Chem.* **1979**, *18*, 327–332.
- (27) Levstein, P. R.; Calvo, R.; Castellano, E. E.; Piro, O. E.; Rivero, B. E. *Inorg. Chem.* **1990**, *29*, 3918–3922.
- (28) Oliva, G.; Castellano, E. E.; Zukerman-Schpector, J.; Calvo, R. *Acta Crystallogr.* **1986**, *C42*, 19–21.
- (29) Gillard, R. D.; Mason, R.; Payne, N. C.; Robertson, G. B. *J. Chem. Soc. A* **1969**, 1864–1871.
- (30) Moussa, S.; Fenton, R. R.; Kennedy, B. J.; Plitz, R. O. *Inorg. Chim. Acta* **1999**, *288*, 29–34.
- (31) Kaitner, B.; Paulić, N.; Pavlović, G.; Sabolović, J. *Polyhedron* **1999**, *18*, 2301–2311.
- (32) Kaitner, B.; Pavlović, G.; Paulić, N.; Raos, N. *J. Coord. Chem.* **1995**, *36*, 327–338.
- (33) Kaitner, B.; Paulić, N.; Raos, N. *J. Coord. Chem.* **1992**, *25*, 337–347.
- (34) Kaitner, B.; Pavlović, G.; Paulić, N.; Raos, N. *J. Coord. Chem.* **1998**, *43*, 309–319.
- (35) Kamenar, B.; Penavić, M.; Škorić, A.; Paulić, N.; Raos, N.; Simeon, V. *J. Coord. Chem.* **1988**, *17*, 85–94.
- (36) Kaitner, B.; Ferguson, G.; Paulić, N.; Raos, N. *J. Coord. Chem.* **1992**, *26*, 95–104.
- (37) Sabolović, J.; Kaitner, B. *Polyhedron* **2007**, *26*, 1087–1097.
- (38) Sabolović, J.; Kaitner, B. *Inorg. Chim. Acta* **2008**, *361*, 2418–2430.
- (39) Krishnakumar, R. V.; Natarajan, S.; Bahudur, S. A.; Cameron, T. S. Z. *Kristallogr.* **1994**, *209*, 443–444.
- (40) Calvo, R.; Levstein, P. R.; Castellano, E. E.; Fabiane, S. M.; Piro, O. E.; Oseroff, S. B. *Inorg. Chem.* **1991**, *30*, 216–220.
- (41) Freeman, H. C.; Snow, M. R.; Nitta, I.; Tomita, K. *Acta Crystallogr.* **1964**, *17*, 1463–1470.
- (42) Weeks, C. M.; Cooper, A.; Norton, D. A. *Acta Crystallogr.* **1969**, *B25*, 443–450.
- (43) Casari, B. M.; Mahmoudkhani, A. H.; Langer, V. *Acta Crystallogr.* **2004**, *E60*, 1949–1951.
- (44) Banci, L. *Curr. Opin. Chem. Biol.* **2003**, *7*, 143–149.
- (45) Hay, B. P. *Coord. Chem. Rev.* **1993**, *126*, 177–236.
- (46) Zimmer, M. *Chem. Rev.* **1995**, *95*, 2629–2649.
- (47) Rappé, A. K.; Casewit, C. J. *Molecular Mechanics Across Chemistry*; University Science Books: Sausalito, CA, 1997.
- (48) Boeyens, J. C. A.; Comba, P. *Coord. Chem. Rev.* **2001**, *212*, 3–10.
- (49) Norrby, P.-O.; Brandt, P. *Coord. Chem. Rev.* **2001**, *212*, 79–109.
- (50) Ledecq, M.; Lebon, F.; Durant, F.; Giessner-Prettre, C.; Marquez, A.; Gresh, N. J. *J. Phys. Chem. B* **2003**, *38*, 10640–10652.

- (51) Nielson, K. D.; van Duin, A. C. T.; Oxgaard, J.; Deng, W.-Q.; Goddard, W. A., III. *J. Phys. Chem. A* **2005**, *109*, 493–499.
- (52) Comba, P.; Remenyi, R. *J. Comput. Chem.* **2002**, *23*, 697–705.
- (53) Comba, P.; Remenyi, R. *Coord. Chem. Rev.* **2003**, *238*, 239, 9–20.
- (54) Deeth, R. J. *Chem. Commun.* **2006**, 2551, 2551–2553.
- (55) Deeth, R. J. *Inorg. Chem.* **2007**, *46*, 4492–4503.
- (56) Deeth, R. J.; Anastasi, A.; Diedrich, C.; Randell, K. *Coord. Chem. Rev.* **2009**, *253*, 795–816.
- (57) Sabolović, J.; Rasmussen, K. *Inorg. Chem.* **1995**, *34*, 1221–1232.
- (58) Sabolović, J.; Liedl, K. R. *Inorg. Chem.* **1999**, *38*, 2764–2774.
- (59) Sabolović, J.; Tautermann, C. S.; Loerting, T.; Liedl, K. R. *Inorg. Chem.* **2003**, *42*, 2268–2279.
- (60) Murphy, B.; Hathaway, B. *Coord. Chem. Rev.* **2003**, *243*, 237–262.
- (61) Siegbahn, P. E. M. *Q. Rev. Biophys.* **2003**, *36*, 91–145.
- (62) Ryde, U. *Curr. Opin. Chem. Biol.* **2003**, *7*, 136–142.
- (63) de Bruin, T. J. M.; Marcelis, A. T. M.; Zuilhof, H.; Sudhölter, E. J. R. *Phys. Chem. Chem. Phys.* **1999**, *1*, 4157–4163.
- (64) Tautermann, C. S.; Sabolović, J.; Voegele, A. F.; Liedl, K. R. *J. Phys. Chem. B* **2004**, *108*, 2098–2102.
- (65) Hattori, T.; Toraishi, T.; Tsuneda, T.; Nagasaki, S.; Tanaka, S. *J. Phys. Chem. A* **2005**, *109*, 10403–10409.
- (66) Berendsen, H. J. C.; Grigera, J. R.; Straatsma, T. P. *J. Phys. Chem.* **1987**, *91*, 6269–6271.
- (67) Tomasi, J.; Mennucci, B.; Cancès, E. *J. Mol. Struct. (THEOCHEM)* **1999**, *464*, 211–226.
- (68) Sabolović, J.; Mrak, Ž.; Koštrun, S.; Janeković, A. *Inorg. Chem.* **2004**, *43*, 8479–8489.
- (69) Niketić, S. R.; Rasmussen, K. *The Consistent Force Field: A Documentation*; Lectures Notes in Chemistry; Springer-Verlag: Berlin, 1977; Vol. 3.
- (70) Rasmussen, K. *Potential Energy Functions in Conformational Analysis*; Lectures Notes in Chemistry; Springer-Verlag: Berlin, 1985; Vol. 37.
- (71) Rasmussen, K.; Engelsen, S. B.; Fabricius, J.; Rasmussen, B. The Consistent Force Field: Development of Potential Energy Functions for Conformational Analysis. In *Recent Experimental and Computational Advances in Molecular Spectroscopy*; Fausto, R., Ed.; NATO ASI Series C: Mathematical and Physical Sciences; Kluwer Academic Publisher: Dordrecht, The Netherlands, 1993; Vol. 406, pp 381–419.
- (72) Williams, D. E. *Top. Curr. Phys.* **1981**, *26*, 3–40.
- (73) Pietilä, L.-O.; Rasmussen, K. *J. Comput. Chem.* **1984**, *5*, 252–260.
- (74) Reed, A. E.; Weinstock, R. B.; Weinhold, F. *J. Chem. Phys.* **1985**, *83*, 735–746.
- (75) Halgen, T. A.; Damm, W. *Curr. Opin. Struct. Biol.* **2001**, *11*, 236–242.
- (76) Lindahl, E.; Hess, B.; van der Spoel, D. *J. Mol. Mod.* **2001**, *7*, 306–317.
- (77) Berendsen, H. J. C.; van Spoel, D.; van Drunen, R. *Comput. Phys. Commun.* **1995**, *91*, 43–56.
- (78) Input Gromacs files with the empirical parameter set are available from J.S. upon request.
- (79) Berendsen, H. J. C.; Postma, J. P. M.; van Gunsteren, W. F.; DiNola, A.; Haak, J. R. *J. Chem. Phys.* **1984**, *81*, 3684–3690.
- (80) Miyamoto, S.; Kollman, P. A. *J. Comput. Chem.* **1992**, *13*, 952–962.
- (81) Becke, A. D. *J. Chem. Phys.* **1993**, *98*, 5648–5652.
- (82) Lee, C.; Yang, W.; Parr, R. G. *Phys. Rev. B* **1988**, *37*, 785–789.
- (83) Vosko, S. H.; Wilk, L.; Nusair, M. *Can. J. Phys.* **1980**, *58*, 1200–1211.
- (84) Stephens, P. J.; Devlin, F. J.; Chabalowski, C. F.; Frisch, M. J. *J. Phys. Chem.* **1994**, *98*, 11623–11627.
- (85) Dunning, T. H., Jr.; Hay, P. J. Gaussian Basis Sets for Molecular Calculations. In *Methods of Electronic Structure Theory*; Schaefer, H. F., III., Ed.; Modern Theoretical Chemistry; Plenum Press: New York, 1977; Vol. 3, pp 1–27.
- (86) Frisch, M. J.; Pople, J. A.; Binkley, J. S. *J. Chem. Phys.* **1984**, *80*, 3265–3269.
- (87) Clark, T.; Chandrasekhar, J.; Spitznagel, G. W.; Schleyer, P. v. R. *J. Comput. Chem.* **1983**, *4*, 294–301.
- (88) Hay, P. J.; Wadt, W. R. *J. Chem. Phys.* **1985**, *82*, 270–283.
- (89) Wadt, W. R.; Hay, P. J. *J. Chem. Phys.* **1985**, *82*, 284–298.
- (90) Hay, P. J.; Wadt, W. R. *J. Chem. Phys.* **1985**, *82*, 299–310.
- (91) Frisch, M. J.; Trucks, G. W.; Schlegel, H. B.; Scuseria, G. E.; Robb, M. A.; Cheeseman, J. R.; Montgomery, J. A., Jr.; Vreven, T.; Kudin, K. N.; Burant, J. C.; Millam, J. M.; Iyengar, S. S.; Tomasi, J.; Barone, V.; Mennucci, B.; Cossi, M.; Scalmani, G.; Rega, N.; Petersson, G. A.; Nakatsuji, H.; Hada, M.; Ehara, M.; Toyota, K.; Fukuda, R.; Hasegawa, J.; Ishida, M.; Nakajima, T.; Honda, Y.; Kitao, O.; Nakai, H.; Klene, M.; Li, X.; Knox, J. E.; Hratchian, H. P.; Cross, J. B.; Bakken, V.; Adamo, C.; Jaramillo, J.; Gomperts, R.; Stratmann, R. E.; Yazyev, O.; Austin, A. J.; Cammi, R.; Pomelli, C.; Ochterski, J. W.; Ayala, P. Y.; Morokuma, K.; Voth, G. A.; Salvador, P.; Dannenberg, J. J.; Zakrzewski, V. G.; Dapprich, S.; Daniels, A. D.; Strain, M. C.; Farkas, O.; Malick, D. K.; Rabuck, A. D.; Raghavachari, K.; Foresman, J. B.; Ortiz, J. V.; Cui, Q.; Baboul, A. G.; Clifford, S.; Cioslowski, J.; Stefanov, B. B.; Liu, G.; Liashenko, A.; Piskorz, P.; Komaromi, I.; Martin, R. L.; Fox, D. J.; Keith, T.; Al-Laham, M. A.; Peng, C. Y.; Nanayakkara, A.; Challacombe, M.; Gill, P. M. W.; Johnson, B.; Chen, W.; Wong, M. W.; Gonzalez, C.; Pople, J. A. *Gaussian 03*, revision C.02; Gaussian, Inc.: Wallingford, CT, 2004.
- (92) Cossi, M.; Scalmani, G.; Rega, N.; Barone, V. *J. Chem. Phys.* **2002**, *117*, 43–54.
- (93) Adamo, C.; Scuseria, G. E.; Barone, V. *J. Chem. Phys.* **1999**, *111*, 2889–2899.
- (94) Adamo, C.; Barone, V. *J. Chem. Phys.* **1999**, *110*, 6158–6170.
- (95) Adamo, C.; Cossi, M.; Scalmani, G.; Barone, V. *Chem. Phys. Lett.* **1999**, *307*, 265–271.
- (96) Peng, C.; Schlegel, H. B. *Isr. J. Chem.* **1993**, *33*, 449–454.
- (97) Peng, C.; Ayala, P. Y.; Schlegel, H. B.; Frisch, M. J. *J. Comput. Chem.* **1996**, *17*, 49–56.



- (98) Albu, T. V.; Corchado, J. C.; Truhlar, D. G. *J. Phys. Chem. A* **2001**, *105*, 8465–8487.
- (99) Warshel, A. *Computer Modeling of Chemical Reactions in Enzymes and Solutions*; John Wiley & Sons, Inc: New York, 1991.
- (100) Åqvist, J.; Warshel, A. *Chem. Rev.* **1993**, *93*, 2523–2544.
- (101) Olsson, M. H. M.; Mavri, J.; Warshel, A. *Philos. Trans. R. Soc. B* **2006**, *361*, 1417–1432.
- (102) Humphrey, W.; Dalke, A.; Schulten, K. *J. Mol. Graphics* **1996**, *14*, 33–38.
- (103) Delf, B. W.; Gillard, R. D.; O'Brien, P. *J. Chem. Soc., Dalton Trans.* **1979**, 1301–1305.

CT9000203